



Coseismic and Aseismic Strain Offsets Recorded by the Gran Sasso Strainmeter

A. Amoruso and L. Crescentini

Dipartimento di Fisica, Università dell' Aquila, I-67100 L'Aquila, Italy

Received 10 May 1996; revised 7 March 1997; accepted 7 April 1998

Abstract. An underground low-noise high-sensitivity laser strainmeter, crossing a fault in the Gran Sasso massif (central Italy), is discontinuously operating since late May 1994, after a few years of mechanical stabilization of end monuments. A swift extensional strain transient reaching a peak of at least $1 \mu\epsilon$ occurred in about one month from the beginning of the operating time, followed by a four-month-long coarsely stable period, and a slower decay. On June 2nd 1994, in coincidence with two local earthquakes, permanent extensional offsets of about $10 \text{ n}\epsilon$ have been recorded. A further aseismic slip of the same order of magnitude and sign has been observed about thirty minutes after the last preceding local event, and ten minutes before the next following one. At the same time, the arrival of seismic waves from a distant earthquake has been recorded by the interferometer. No similar signal behaviour has been observed any more since then.

© 1999 Elsevier Science Ltd. All rights reserved.

1 Introduction

In the mid-eighties, in coincidence with the escavation of a highway tunnel under the Gran Sasso mountain, an underground laboratory, mainly devoted to high-energy physics, has been realized in central Italy (Istituto Nazionale di Fisica Nucleare - Laboratorio Nazionale del Gran Sasso, see Fig. 1). This occurrence has given a chance to install a geophysical interferometer (Fiocco et al., 1986) 5 km from each entrance of the tunnel, more than 250 m aside from the highway, and at least 1100 m under the free surface, taking advantage of the tunnels that surround the main halls, where an important normal fault (strike = $N25^\circ E$, dip = $40^\circ N$) is situated. Such tunnels, which constitute an outer by-pass of the experimental halls, were extended to constitute a triangle. Two orthogonal sides of the triangle, each about

Correspondence to: L. Crescentini

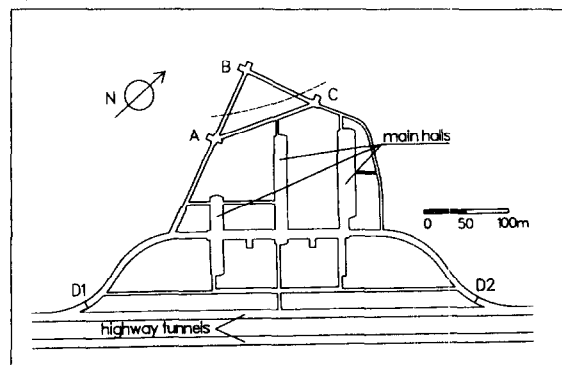


Fig. 1. Map of the underground laboratory. End monuments of the interferometer are located in A, B, and C. The dashed line roughly represents the fault crossed by the interferometer.

90 m long, are crossed at half-way by the fault (dashed line in Fig. 1), which at a slant angle separates more rigid dolomites from more plastic limestones. This fault, whose tilted plane crosses the vertical of the halls at a distance of the order of hundred meters, constitutes an important feature in the complex geology of the Gran Sasso mountain, and is expected to have some modest level of activity (Calembert et al., 1972). The geographical co-ordinates of the underground laboratory are: $42^\circ 27.66' N$, $13^\circ 33.87' E$, 962 m altitude. In the present configuration, the main arm of the instrument is oriented along an axis approximately $N24^\circ W$

2 Experimental setup

The interferometer was planned to measure relative displacements of three 1 m^3 concrete blocks located in A, B, and C (see Fig. 1) each sitting on a 8 m^3 underground cubic platform. The platforms are embedded in the rock and separated from the tunnel floor by

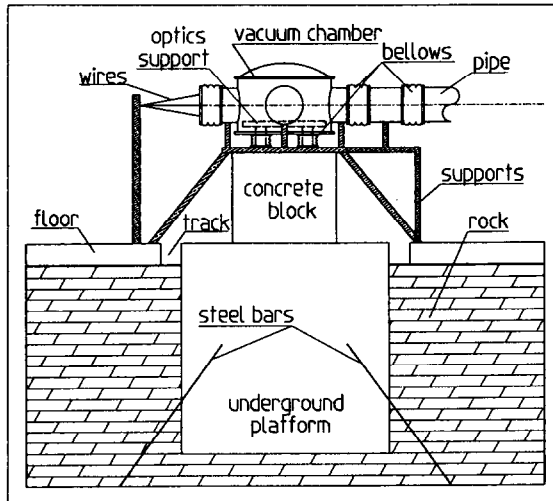


Fig. 2. Sketch of end monuments and supporting structures.

means of a 20 cm wide track. End monuments have been built about ten years ago, so that mechanical relaxation processes should have come to an end. Until October 1995, the interferometer has been working in an unequal-arm configuration, using a 90 m long measurement arm (BC in Fig. 1) and a 50 cm long reference arm. As usual, the interferometer works in an evacuated environment. Optical components are firmly attached to the concrete blocks but to some extent uncoupled from the vacuum chambers by means of bellows (see Fig. 2). A temperature controlled building has been built around monument B , where the laser source and the electronics are kept. Temperature inside the building is maintained at 291 ± 0.1 K. Room temperature in the tunnels is naturally fixed at about 280 ± 0.4 K. Continuous monitoring of air temperature and pressure inside the building and of air temperature in the tunnels is carried out by four solid state thermometers and one capacitive pressure transducer. The optical apparatus is shown in Fig. 3. It is an improved version of a laboratory prototype already described in Crescentini and Renzella (1991) and it will be only briefly described here. A collimated beam of light from a He-Ne laser source L (wavelength $\lambda = 0.6328 \mu\text{m}$) is sent to a beamsplitter B , where it divides equally and goes to two retroreflectors C_1 and C_2 , at the end of the reference and measurement arms respectively. The returned beams meet and interfere at B , going in part to detector P_1 and in part to detector P_2 . The reference arm includes a transverse field electro-optical phase modulator. An analog electronic feedback causes the optical length of the phase modulator to change in time in order to maintain a fixed phase delay, around 45° , between the reference and the measurement beams.

In order to extend the dynamic range of the instrument, limited by the maximum voltage that can act on

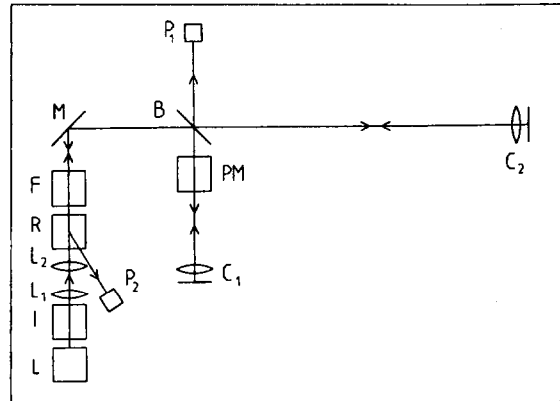


Fig. 3. Optical set-up of the interferometer: L , laser source; I , optical isolator; L_1 , L_2 , collimating lenses; R , Rochon prism; F , Faraday rotator; M , alignment mirror; B , beam-splitter; PM , phase modulator; C_1 , C_2 , retroreflectors; P_1 , P_2 , photodiodes.

the electro-optical modulator, a reset circuit has been included, capable of changing the optical length of the phase modulator by $\pm\lambda$, each time the pathlength difference ΔL reaches $\mp\lambda/2$.

The retroreflector in each of the two arms is a "cat's-eye" (lens and mirror) which minimizes beam distortion and alignment difficulties. This causes the reflected beam to overlap the incident beam, making it necessary to separate the two beams again between the beam-splitter and the laser, and requiring an extremely good isolation of the laser itself from the returning light.

Voltage applied to the phase modulator is sampled by a 12-bit digital-to-analog converter, able to transfer data to a PC through direct memory access (DMA). Unfortunately, wide strain oscillations around 100 Hz, maybe due to mechanical resonances of the tunnel covering, are present. Since their amplitude can be as large as 2 ne , and hence larger than the hysteresis of the reset circuit, a 6 kHz sampling rate is used. Two memory buffers are alternatively used in input. While one of the two buffers is acquiring, data stored in the latter are digitally filtered using a linear nonrecursive filter, decimated at 20 Hz, and preanalyzed. Depending on how fast strain changes in time, data are more and more filtered, and recorded at a rate variable from 0.5 to 20 Hz.

The nominal resolution of this instrument is 3 pe , though the actual capability of detecting geophysical signals is limited by the noise of the site. During the first working year a few breaks occurred, in order to improve the instrument; however, the interferometer suffered only one failure.

3 Strain offset measurements

A typical set of raw data is shown in Fig. 4: both periodic, e.g. earth tides and teleseisms, and aperiodic sig-

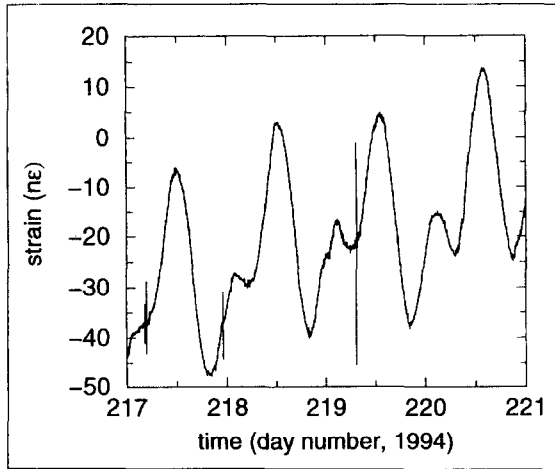


Fig. 4. Typical raw data recorded at variable rate.

nals are evident. Figure 5 shows strain data from May 1994 to July 1995, after filtering and decimating them at one sample every 600 s; the apparent large noise at periods of a few days to one week is due to tidal beats. The interferometric technique makes the actual starting value for each strain record intrinsically unknown; thus subsequent files have been joined by fitting a sum of earth tides, a low-order polynomial, and one strain step on experimental data.

During the first month a swift increase in the baseline up to about $1 \mu\epsilon$ was observed. After a four-month-long period of coarse stability, a slower rebound followed. In order to explain such a pattern more data are needed, however it is neither due to seasonal effects, as proved by the reversed trend in May to July 1995 with respect to May to July 1994, nor caused by mechanical relaxation processes. Comparison with room pressure and temperature rejects any correlation among them and the overall strain pattern. This latter resembles stress evolution as predicted by Bonafede and Albarello (1992) for stress diffusion across the Adriatic microplate, due to dislocation events occurred in the Dinaric region.

Migration of land deformation was observed several years ago (Kasahara, 1979, e.g.), but the effects of precipitation on crustal strain, even as regards long-period fluctuations, have subsequently been stressed (Kasahara et al., 1983). A preliminary comparison of our data with rainfalls at one of the entrances of the highway tunnel shows no correlation with the strain pattern; however, before drawing any conclusion, at least snow load on the mountain and the depth of the aquifer should be considered. At the moment, these data are not available, but the depth of the aquifer near the underground laboratories and the highway tunnels is kept at an almost constant level by continuous draining.

On June 2nd, 1994, during the swift extension period, a swarm of local earthquakes occurred, including

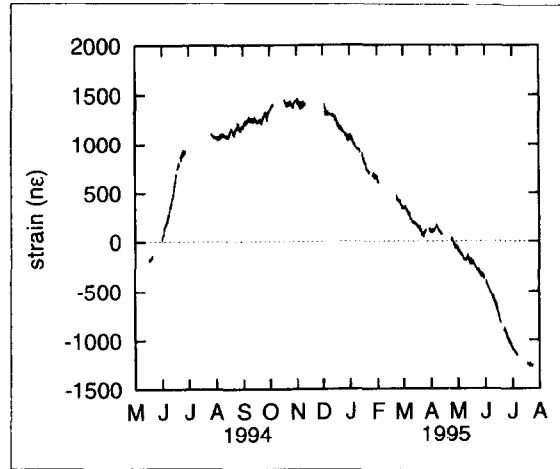


Fig. 5. Strain from May 1994 to July 1995; experimental data have been filtered and decimated at one sample every 600 s.

the only ones in the period May 1994 to July 1995 having epicentral distances from the interferometer shorter than 50 km and magnitude higher than 2.5. The two largest events were M_L 3.5 and M_L 3.3. Two extensional strain offsets were recorded on the interferometer during these same shocks, respectively 4 nε and 16 nε in amplitude (see Fig. 6). Their amplitudes are compatible with theoretical estimates by Dobrovolskiy (1992) for earthquakes having similar magnitude, depth, and epicentral distance; moreover, an enhancement of coseismic effects could be due to the fault crossed by the interferometer. Unfortunately, till summer 1994 high-frequency signals were filtered out during the acquisition process, and it is impossible either to know the amplitude of the transitory seismic wave strain or to exclude spurious behaviors in the strainmeter. This limit induced us to use a variable rate acquisition (up to 20 Hz, see Sect. 2), but the lack of later comparable local events makes any validation impossible.

A subsequent extensional aseismic slip, approximately 6 minutes in duration and 8 nε in amplitude, was observed about 90 minutes after the second coseismic offset, 30 minutes later than the preceding minor local event, and 10 minutes before the following one (the magnitude threshold of the local catalogue is about 1). At the same time, the arrival of seismic waves due to a $M_B=5.5$ $M_{S_z}=7.2$ earthquake near Jawa was recorded by the interferometer (see Fig. 7). In this last case we can exclude any spurious effect since many wider teleseismic waves have been recorded on the interferometer, and no similar behavior has been observed, nor any evidence of instrumental hysteresis has been found. The largest one was the $M_B=6.4$ $M_{S_z}=7.6$ Honshu earthquake occurred on December 28th 1994, which produced a strain signal twenty-times as large in amplitude as the Jawa earthquake (see Fig. 8). Future work will

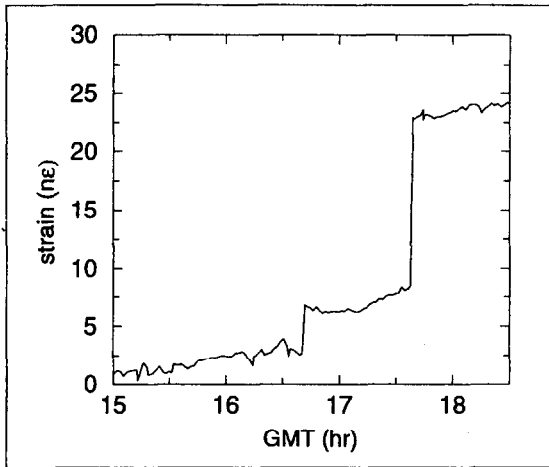


Fig. 6. Coseismic offsets recorded in coincidence with the two major events occurred on June 2nd, 1994.

be devoted to confirm previous reported observations.

Acknowledgements. Thanks are due to D. Albarello and M. Bonafede for useful discussions and to P. Monacelli, Director of Laboratorio Nazionale del Gran Sasso, for logistic support.

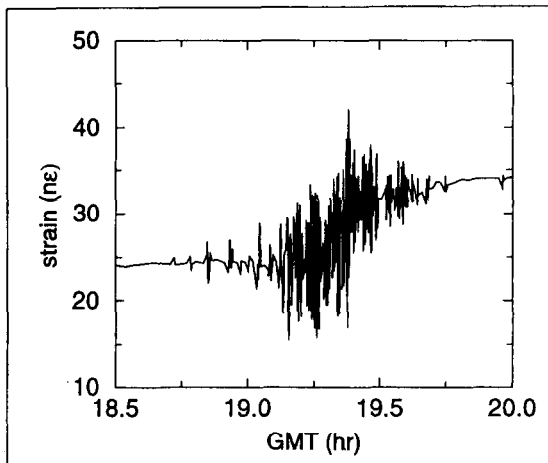


Fig. 7. Signal recorded during the transit of teleseismic waves produced by a $M_s=7.2$ earthquake near Jawa (June 2nd, 1994).

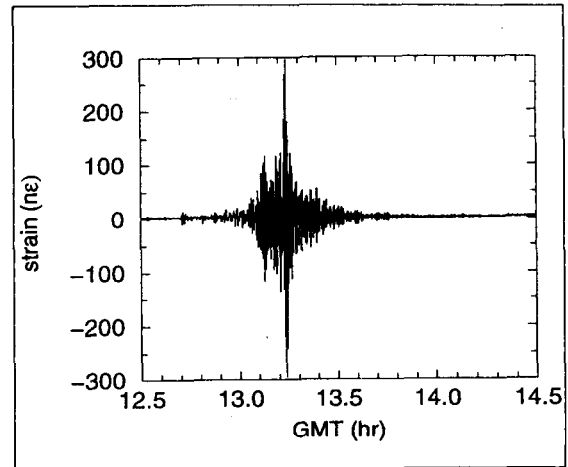


Fig. 8. Signal recorded during the transit of teleseismic waves produced by a $M_s=7.6$ earthquake near Honshu (December 28th, 1994).

References

- Bonafede, M. and Albarello, D., Interaction between microplate boundaries and its effect on seismic activity, *Earthquake Prediction*, M. Dragoni and E. Boschi (eds.), Editrice Il Cigno - Galileo Galilei, Rome, 199-224, 1992.
- Calembert, L., Catalano, P. G., Conato, A., Lambrecht, V., and Mojoie L., Observations dans le massif du Gran Sasso, *C. R. Acad. Sci. Paris*, 274, 2013-2018, 1972.
- Crescentini, L. and Renzella, G., A wide-band high-sensitivity laser strainmeter, *Rev. Scient. Instrum.*, 62, 1206-1209, 1991.
- Dobrovolskiy, I. P., Analysis of preparation of a strong tectonic earthquake, *Izvestiya Earth Physics*, 28, 481-493, 1992.
- Fiocco, G., Visconti, G., and Catalano, P. G., Interferometria laser per la misura delle deformazioni della crosta terrestre: progetto della stazione del Gran Sasso, *Il Nuovo Saggiatore*, 4, 25-28, 1986.
- Kasahara, M., Migration of crustal deformation, *Tectonophysics*, 52, 329-341, 1979.
- Kasahara, M., Shichi, R., and Okada, Y., On the cause of long-period crustal movement, *Tectonophysics*, 97, 327-336, 1983.